Atmos. Chem. Phys. Discuss., 7, 10589–10629, 2007
www.atmos-chem-phys-discuss.net/7/10589/2007/

Atmospheric Chemistry and Physics Discussions

PM speciation and sources in Mexico during the MILAGRO-2006 Campaign

X. Querol[1], J. Pey[1], M. C. Minguillón[1], N. Pérez[1], A. Alastuey[1], M. Viana[1], T. Moreno[1], R. M. Bernabé[2], S. Blanco[2], B. Cárdenas[2], E. Vega[3], G. Sosa[3], S. Escalona[3], H. Ruiz[3], and B. Artíñano[4]

[1]Instituto de Ciencias de la Tierra "Jaume Almera", CSIC. C/ Lluís Solé i Sabarís s/n, 08028 Barcelona, Spain
[2]Centro Nacional de Investigación y Capacitación Ambiental, CENICA. Periférico 5000, Col. Insurgentes Cuicuilco, C.P. 04530, Delegación Coyoacán, México D.F., Mexico
[3]Instituto Mexicano del Petróleo, Eje Central Lázaro Cárdenas 152, Col. San Bartolo Atepehuacan. Delegación Gustavo A. Madero. 07730, México, D.F, Mexico
[4]CIEMAT, Avda. Complutense 22, 28040 Madrid, Spain

Received: 5 July 2007 – Accepted: 18 July 2007 – Published: 23 July 2007

Correspondence to: X. Querol (xavier.querol@ija.csic.es)

Abstract

Levels of PM_{10}, $PM_{2.5}$ and PM_1 and chemical speciation of PM_{10} and $PM_{2.5}$ were measured during the MILAGRO campaign (1 to 31 March 2006, but extended in some cases until 6 April) at four urban, one suburban, two rural, two rural background sites with different degree of industrial influence in the Mexico City Metropolitan Area (MCMA) and adjacent regions. PM_{10} and $PM_{2.5}$ daily levels varied between 50–56 $\mu g/m^3$ and 24–46 $\mu g/m^3$ at the urban sites, 22–35 $\mu g/m^3$ and 13–25 $\mu g/m^3$ at the rural sites, and 75 $\mu g/m^3$ and 31 $\mu g/m^3$ at the industrial hotspot, respectively; lower than those recorded at some Asian mega-cities and similar to those recorded at other South American cities. At the urban sites, hourly $PM_{2.5}$ and PM_1 concentrations showed a marked impact of road traffic emissions (at rush hours), with levels of coarse PM remaining elevated during daytime. At the suburban and rural sites, different PM daily patterns were registered according to the influence of the pollution plume from MCMA and also on local soil resuspension.

The speciation studies showed that mineral matter accounted for 25–27% of bulk PM_{10} at the urban sites and a higher proportion (up to 43%) at the suburban and rural sites. This pattern is repeated in $PM_{2.5}$, with 15% at urban and 28% at suburban and rural sites. Carbonaceous compounds accounted for a similar proportion at the urban sites (24–32% in PM_{10}, and up to 37% in $PM_{2.5}$), markedly reduced at the suburban and rural sites (17% in PM_{10}, and 23–38% in $PM_{2.5}$). The secondary inorganic aerosols accounted for 10–20% of bulk PM_{10} at urban, suburban, rural and industrial sites, with a higher proportion (40%) at the industrial background site. A relatively high proportion of nitrate in rural sites was present in the coarse fraction.

Typically anthropogenic elements (As, Cr, Zn, Cu, Pb, Sn, Sb, Ba, among others) showed considerably high levels at the urban sites; however levels of particulate Hg and crustal trace elements (Rb, Ti, La, Sc, Ga) were generally higher at the suburban site.

Principal component analysis identified three common factors: crustal, regional

ACPD

7, 10589–10629, 2007

background and road traffic. Moreover, some specific factors were obtained for each site.

1 Introduction

During the last few decades a large number of epidemiological studies have shown a link between pollution by airborne particulate matter (PM) and respiratory and cardiovascular disease (Dockery et al., 1993; Künzli et al., 2000; WHO, 2003). Because a lower threshold under which no health effects are observed cannot be determined (WHO, 2003 and 2005), toxicological studies are currently aiming to identify which particle characteristics are responsible for which adverse health effects (e.g., particle number, size, surface, chemical composition). Anthropogenically emitted particulate matter (PM) is generally considered to pose the largest threat to human health given its small grain-size, although the effects of naturally emitted PM (wind-blown dust, sea salt) cannot be discarded (CAFE, 2004, Pérez et al., 2007[1]).

PM air pollution in urban agglomerations comes mostly from anthropogenic sources (i.e. traffic, industrial processes, energy production, domestic and residential emissions, construction), but there is also a minor contribution from natural sources (e.g. bioaerosols, soil dust, marine aerosol, volcanic eruptions). Once emitted into the atmosphere, this complex mixture of pollutants may be transformed as a function of the ambient conditions and the interaction among different PM components, as well as gaseous pollutants. The PM system is especially complex in mega-cities due to:

- Large emission volumes of PM components and gaseous precursors.
- High variability of sources.

[1]Pérez, L., Tobias, A., Querol, X., Alastuey, A., Viana, M., Pey, J., González-Cabré, M., Valero, N., Künzli, N., and Sunyer, J.: Saharan dust outbreaks increases mortality in Barcelona (Spain), J. European Epidemiology, submitted, 2007.

– Widespread distribution of emission sources.

– Possible long-range transport of the polluted air masses.

The WHO/UNEP report on air quality in 1992 focused on 20 mega-cities of the world, which were defined as urban agglomerations with populations of 10 million or more by the year 2000 (WHO/UNEP, 1992). The list of mega-cities included not only Tokyo, Mexico City, Cairo, Bangkok or Beijing, but also Los Angeles, New York and London. Monitoring air quality in large urban agglomerations is a pressing need in order to ensure the health and well being of urban residents, but it is also essential if we intend to prevent air pollution-related problems from occurring in emerging mega-cities which may influence both air quality and climate change on the regional, continental and global scales (Molina et al., 2007). Preventing pollution problems before they occur is usually the most cost-effective method for dealing with air pollution.

In order to better understand the evolution of trace gases and particulates originating from anthropogenic emissions in Mexico City and their impact on regional air quality and climate, a field campaign called the Megacities Initiative: Local And Global Research Observations (MILAGRO, http://www.eol.ucar.edu/projects/milagro/) collected a wide range of meteorological, chemical, gaseous and particulate measurements during March 2006. The design of this campaign was partly based on the results obtained during the MCMA-2003 Campaign (Salcedo et al., 2006; Volkamer et al., 2006; Molina et al., 2007; Zhang et al., 2007), during which exploratory field measurements of ambient aerosols were carried out in Mexico City. This campaign helped in defining physical and chemical properties of the aerosols, as well as the dominant meteorological scenarios in this mega-city, on which the current MILAGRO campaign were based. During the MILAGRO campaign measurements were obtained over a wide range of spatial scales from local, regional, and large-scale field experiments to describe the evolution of the Mexico City pollutant plume from its source and up to several hundred kilometers downwind.

The present study deals with the speciation and source apportionment of TSP, PM_{10}

and $PM_{2.5}$ in the Mexico City Metropolitan Area (MCMA), by means of an intensive sampling campaign (1 March to 6 April 2006) of measurement, sampling and analysis of PM integrated into the 2006 MILAGRO campaign. The main goal of the present study is to interpret the variability of PM levels and composition (including trace metals) in Mexico City, as well as to identify the major emission sources (of PM and trace metals) in the area.

2 Methodology

2.1 Measurements and sampling

Measurement and sampling of PM were carried out at the following monitoring stations (Table 1 and Fig. 1):

T0. This monitoring station is located to the northwestern part of the basin of Mexico City. It is an urban background site influenced by road traffic fresh emissions (300 m from four major roads surrounding it), domestic and residential emissions, but also potentially influenced by local industrial emissions and from the Tula industrial area (around 60 km to the north-northwest, in the Hidalgo State). This station was equipped with high volume samplers fitted with cut off inlets for PM_{10} (Wedding, 68 m^3/h) and $PM_{2.5}$ (MCV, 30 m^3/h) from 1 March to 4 April 2006 (n=35, 12 h integrated samples), and 6 to 29 March 2006 (n=24, 12 h integrated samples), respectively. This monitoring site was also equipped with a laser spectrometer (GRIMM 1107, US1) for real time measurement of hourly levels of PM_{10}, $PM_{2.5}$ and PM_1, from 19 to 30 March 2006.

CENICA. This is an urban background station, with similar characteristics to T0, but located in the southeastern side of the city of Mexico. This station was equipped with a high volume sampler fitted with a cut off inlet for PM_{10} (Wedding, 68 m^3/h) from 1 March to 6 April 2006 (n=38, 12 and 24 h integrated samples). This monitoring site was also equipped with a laser spectrometer (GRIMM 1108) for real time measurement of hourly levels of TSP, PM_{10}, $PM_{2.5}$ and PM_1, from 8 to 29 March 2006.

ACPD
7, 10589–10629, 2007

UNAM. This is an urban background station, influenced by road traffic and residential emissions, with similar characteristics to T0 and CENICA, but located on the southern side of the city of Mexico. This station was equipped with a high volume sampler and a cut off inlet for PM_{10} (Wedding, 68 m^3/h) from 1 to 15 March 2006 (n=7, only 24 h samples).

Jasso (Subestacion) and PXT. These two regional background sites were located in the vicinity of a heavy industrialized area, the Tula-Vito-Apasco industrial corridor, 60 km north-northwest from the Mexico City downtown. Jasso and PXT were 6 km southwest and 25 km south from a large refinery and a power plant (Tula estate). At the two sites PM_{10} and $PM_{2.5}$ samples were collected by using portable low volume samplers (MiniVol) operating at a flow rate of 0.3 m^3/h and previously calibrated under standard conditions. Samples were collected from 00:00 to 24:00 h each day from 24 of March to 20 April 2006, with a total number of samples of n=55 for PM_{10}, and n=55 for $PM_{2.5}$. Additionally, medium volume sequential filter samplers (SFS) operated at a flow rate of 6.8 m^3/h and equipped with $PM_{2.5}$ inlets were used to collect 12-h samples from 7 to 20 April 2006 (n=56).

T1. This is a suburban background site located around 50 km to the north of México City, in an area isolated from major urban agglomerations but close to small populated agglomerations, and around 500 m from the closest road. The station was equipped with three high volume samplers (Wedding, 68 m^3/h) with TSP, PM_{10} and $PM_{2.5}$ cutoff inlets from 1 to 29 March 2006 (n=25, 24 and 23, 12 h integrated samples respectively).

T2. This is a regional background site located around 90 km to the north of the city of Mexico, in the surroundings of a farm isolated from major urban agglomerations, and around 2 km from the closest road. The monitoring site was equipped with a Wedding high volume (68 m^3/h) sampler with a PM_{10} cut off inlet from 9 to 17 March 2006 (n=8).

CORENA and TENANGO. At these urban background and regional background sites, respectively, two laser spectrometers (GRIMM 1107) for real time measurements of levels of PM_{10}, $PM_{2.5}$ and PM_1, were installed from 1 to 4 April 2006 at CORENA and 28 March to 7 April 2006 at TENANGO.

ACPD
7, 10589–10629, 2007

EGU

The main objective of the measurements performed at the urban background sites was the characterization and source apportionment of urban aerosols in MCMA. Elucidation of the origin of particulate mercury in PM_{10} was of particular interest here. In contrast, the main objective of data collection at the regional background site was to investigate the influence of the emissions from MCMA on the composition of the atmospheric aerosols in the surrounding rural sites.

Samples from T0, T1, T2, UNAM and CENICA obtained with the high volume samplers were collected at all sites on quartz micro-fiber filters (Pallflex for the Wedding instruments and Schleicher & Schuell for the MCV instruments), conditioned for subsequent analysis. High volume samplers were operated one out of every two days along the field campaign. Two 12 h samples were collected every sampling day (from 08:00 h to 20:00 h and 20:00 h to 08:00 h local time), with the exception of UNAM and T2 (24 h samples).

Samples from Jasso and PXT sites were collected on 47 mm Teflon-membrane (2 μm pore size, Gelman Scientific, Ann Arbor, MI, USA) and quartz-fiber (Pallflex Products Corp., Putnam, CT, USA) filters. Teflon filters were used for mass analyses, trace element analyses and light transmission, whereas quartz filters were used for ion, elemental and organic carbon analyses.

Real time measurements of PM obtained with the laser spectrometer were compared and corrected versus gravimetric measurements obtained with the high volume samplers.

2.2 Chemical and microscopy analysis

Samples were conditioned after sampling (50±4% humidity and 22±3°C during 48 h) prior to gravimetric determination of the PM mass. Levels of major and trace elements were determined in bulk sample acidic digestions ($HF:HClO_4:HNO_3$) by means of Inductively Coupled Atomic Emission Spectrometry (ICP-AES) and Inductively Coupled Plasma Mass Spectrometry (ICP-MS), respectively. Levels of particulate mercury were determined by means of a Hg Gold Amalgam Atomic Absorption analyzer

ACPD
7, 10589–10629, 2007

(AMA-LECO). The content of soluble ions (Cl^-, SO_4^{2-}, NO_3^- and NH_4^+) was determined by means of Ion Cromatography and colorimetry-FIA. Total Carbon was determined by means of a LECO elemental analyzer. OC and EC levels were determined on a selected number of samples to determine the ratios OC/EC by Thermo-Optical Reflectance (TOR) according to the method described by Fung et al., (2002). Sample treatment and analytical details are described in Querol et al. (2001). Indirect determinations from analytical data were obtained for: a) CO_3^{2-}, determined from Ca content, assuming that this element is mainly present as calcite ($CaCO_3$; CO_3^{2-} = 1.5*Ca); b) SiO_2, determined from the Al content on the basis of prior experimental equations (SiO_2=3*Al_2O_3; Querol et al., 2001). Selected samples were also studied under an environmental Scanning Electron Microscope (SEM, FEI QUANTA 200), with chemical analyses of individual particles being performed manually on uncoated samples using an energy dispersive X-ray microanalysis system (EDX). Microscope conditions were working distance of 10 mm, accelerating voltage of 20 kV, a beam spot size of 2 μm with a beam current of approximately 1.00 μA, and a spectrum acquisition time of 30 s live time, with particles being analyzed in its centre.

2.3 Meteorological data

At T0 site, a 3-D sonic anemometer (Campbell Scientific, model CSAT3) was used to measure horizontal and vertical wind components at 1 Hz. Temperature, relative humidity and atmospheric pressure were registered using Vaisala HMP-series sensors. All the equipment were deployed at 12 m above the ground level. Data was kindly made available for MILAGRO participants by W. Eichinger from the University of Iowa.

3 Atmospheric dynamics

Mexico City is located in an elevated basin, 2240 m above mean sea level (m a.s.l.). Surrounding mountains on the west, south and east reach 1000 m above the basin,

and two volcanoes at the southeast reach over 5000 m a.s.l. The basin is opened to the north and southeast, where a small gap between mountains allows entering of cold and fresh air during evenings, cleaning up the basin most of the time.

Fast and Zhong (1998) emphasize the importance of vertical mixing and mountain winds in the transport of the Mexico City urban plume first towards the south during the day and then back over the city to the north during nightime. Clear skies, low humidity, and weak winds aloft associated with high-pressure systems are usually observed over Mexico during March (Fast et al., 2007).

Based on MILAGRO field measurements and large-scale analyses Fast et al. (2007) defined three regimes that characterized the overall meteorological conditions: before 14 March, between 14 and 23 March, and after 23 March. Mostly sunny and dry conditions with periods of cirrus and marine stratus along the coast occurred during the first regime. The beginning of the second regime was characterized by a sharp increase in humidity over the central plateau and the development of late afternoon convection associated with the passage of a weak cold front on 14 March. The third regime began with the passage of a strong cold front that lead to humidity, afternoon convection, and precipitation over the central plateau that was higher than during the second regime. The frequency and intensity of fires, as determined by satellite measurements, also diminished significantly after the third cold surge.

Fast et al. (2007) reported that during 1 to 8 March 2006, high pressure at 700 hPa (3200 m a.s.l.) slowly moved from northwestern Mexico towards the east so that the winds over Mexico City were from the north and east. These synoptic conditions would transport Mexico City pollutants towards the Pacific Ocean. However, the clockwise circulation resulting from the high pressure scenario would eventually transport these pollutants back over Mexico. An upper-level trough propagating through the south-central U.S. on 9 March produced westerly winds over Mexico. The winds became southwesterly between 10 and 12 March as a trough developed over the western U.S. After this trough moved over the north-central U.S. on 13 March, the winds over central Mexico became light and variable. Between 14 and 18 March a series of troughs and

ridges propagated from west to east across the U.S. that affected the position of the high-pressure system over the Gulf of Mexico and lead to variable wind directions over central Mexico. A stronger trough propagated into the south-central U.S., producing stronger southwesterly winds between 19 and 20 March. After 21 March, high pressure gradually developed over southern Mexico that produced westerly winds at this level over central Mexico for the rest of the month. Wind speeds exceeding 15 m/s at 500 hPa were associated with the troughs during the 9–11 March and 19–20 March periods. Wind speeds at 700 hPa were almost always less than 10 m/s and usually less than 5m/s.

According to Doran et al. (2007), on 10, 18, 19, 20, 22, and 24 March T1 and T2 were influenced by the Mexico's emission plume. This type of air mass circulation coincides with that reported by Molina et al. (2007) during episodes of ozone transport towards the northeast from MCMA.

4 Results

4.1 PM levels

Table 2 summarizes the mean TSP, PM_{10}, $PM_{2.5}$ and PM_1 levels measured at the different monitoring stations. Although the measuring periods were not simultaneous at all the monitoring sites, it is evident that the mean PM_{10} levels measured at the urban background sites of Mexico City for the study period fall in a narrow range, from 50 to 56 $\mu g/m^3$, the values from real time and gravimetry being very similar. For $PM_{2.5}$ and PM_1 a wider range of levels was measured, with 24 to 40 and 19 to 33 $\mu g/m^3$, respectively. At the Jasso industrial hotspot PM_{10} levels measured increased up to 75 $\mu g/m^3$, although $PM_{2.5}$ levels (31 $\mu g/m^3$) were in the range defined for Mexico City (35 $\mu g/m^3$) (Vega et al, 2004). At the rural sites PXT and T2 PM levels fall within the range 34 to 37 $\mu gPM_{10}/m^3$ and 26 $\mu gPM_{2.5}/m^3$. Levels at the suburban site T1 (193, 82 and 33 $\mu g/m^3$ for TSP, PM_{10} and $PM_{2.5}$) and the regional background site Jasso (75

and 31 μg/m^3 for PM_{10} and $PM_{2.5}$, respectively) were markedly higher probably due to intensive local soil dust resuspension and to the influence of a cement plant and limestone quarry at Jasso. It should be noted that at the urban sites, the instrumentation was located on the terrace of buildings and that PM concentrations at ground level would probably be much higher.

Although the above PM levels may be considered as relatively high when compared with the US or European air quality standards, they are markedly lower than PM levels measured at Asian mega-cities (or large cities). Thus, as shown in Table 3, most large cities in China and India record annual mean levels of 80–150 μgPM_{10}/m^3 and 60–125 μg$PM_{2.5}$/m^3. Moreover, data reported by Clean Air Initiatives for Asian cities (2006) show that, with the exception of Tokyo, most Asian mega-cities (>10 million population) and large cities exceed 100 μgPM_{10}/m^3 as a mean annual average (mean 2005 annual levels in μgPM_{10}/m^3: 51 Bangkok; 155 Beijing; 115 Hanoi, 80 Jakarta; 110 Calcutta; 80 Mumbai; 160 New Delhi; 70 Seoul; 100 Shanghai; 35 Tokyo). These levels are up to 3 times higher than those recorded in Mexico City during the MILAGRO campaign, although it must be taken into account that the PM concentrations presented in this study are not annual means, as it is the case for the Asian cities described above.

Similar levels of PM_{10} were measured at the two urban background sites with the largest data coverage (CENICA and T0), with a simultaneous variation in the levels of PM measured at both sites (α=1.0, R^2=0.9: see Fig. 2). Daylight 12 h PM_{10} levels were similar (α=1.0, R^2=0.6). The variation of PM_{10} levels was even better synchronized at the two sites during the night (R^2=0.9), although 20% higher values (α=0.8) were recorded at T0. The higher night-time values at T0 could be related to aged pollutant transport towards the north, as described by Fast and Zhong (1998). These results indicate that both stations are indeed representative of urban background PM_{10} climate in Mexico City, and that PM_{10} levels varied on a relatively large scale during the MILAGRO campaign. The lower diurnal correlation of the PM_{10} levels is probably attributable to the influence of soil resuspension at CENICA. In this context, an important difference between the relative contributions of coarse and fine PM was detected.

PM_{10} at CENICA had a larger proportion of coarse PM (50% $PM_{2.5-10}$) whereas at T0 the finer fraction was dominant (only 30% $PM_{2.5-10}$), probably due to higher traffic exhaust emissions in the vicinity of T0.

At the suburban and rural sites the coarse fraction accounted from 30 to 60% of the PM_{10} mass. This large variation in the relative proportion of fine and coarse fraction is due to a high impact of local soil resuspension at T1 and to resuspension of dust from a nearby cement plant and limestone quarry at Jasso. At T1 and Jasso sites, these large resuspended dust contributions accounted for high levels of PM_{10} and $PM_{2.5}$, when compared with the other rural sites (by a factor of 2 to 4).

The hourly evolution of PM levels measured during the entire MILAGRO campaign at the urban background sites of Mexico City, CENICA and T0 (Fig. 3), was most strongly influenced by the peak fine PM concentrations recorded during the morning traffic rush hours. The coarse fraction increased also at morning rush hours, remaining high and reaching the maximum at 16:00–18:00 h, followed by a nightly decrease (less urban dust resuspension). The 2 monitoring sites followed the same mean daily pattern, with a very clear afternoon coarse PM peak, probably attributable to the higher wind speed typically recorded at Mexico City during the afternoon in this period of the year (Fig. 4).

At the two sites located to the South of Mexico City, different PM daily trends were recorded, with the maximum PM being registered in the afternoon, at 19:00 h at Tenango and at 14:00 h at Corena. This is probably due to the transport of the urban plume from México, which reaches Corena (south) at 14:00 h and Tenango (southeast) at 18:00–19:00 h. Both fine and coarse fractions are affected by this transport. This is supported by the measurements at the rural site Tenango plotted in Fig. 5, showing Mexico City's plume impact causing high levels of PM_1 during the period 15-21 h and much reduced over the rest of the day.

As expected, PM_{10} levels were at all sites higher (by a factor around 1.3) during daylight, as a consequence of the higher atmospheric emissions and turbulence. This difference was much reduced in the case of $PM_{2.5}$.

Concerning the daily evolution of PM levels measured at the two urban background

sites, CENICA and T0 (Fig. 6), two definite periods can be clearly identified. The first one lasted from the beginning of the measurements until 23 March, and was characterized by relatively high levels of PM_{10} (a mean of 57 $\mu g/m^3$), with a dominant coarse grain size ($PM_{2.5-10}$ and PM_{1-10} loads were 57% and 67% of bulk PM_{10}) due probably to the influence of resuspension of urban dust. The second period started on 23 March and lasted until the end of the month, and was characterized by lower PM_{10} levels (35 $\mu g/m^3$) and a finer grain size ($PM_{2.5-10}$ and PM_{1-10} loads were 41% and 50% of bulk PM_{10}). This was coincident with the last meteorological period of the field campaign when precipitation was frequent and the resuspension of urban dust diminished. This wet period also influenced $PM_{2.5}$ and PM_1 levels which slightly decreased (by 18%), but not as much as PM_{10} (by 40%). In addition to the above described mean hourly patterns (defined by road traffic emissions and wind velocity/dust resuspension), two additional types of PM episodes were identified. One from 04:00 to 06:00 h with relatively high levels of PM_1 occurring on 14, 18, 21, 22 and 25 to 27 March 2006. During most of those days, $PM_{2.5}$ levels were higher during the night than during daytime. These episodes are also reflected in the mean hourly evolution obtained for the urban sites (Figure 3), and as interpreted already by Doran et al. (2007) on the basis of real time measurements of OC and EC at T1 and T2, they may be attributed to the trapping of pollutants in the Mexico City area overnight and during the morning hours in a shallow surface layer before the rapid growth of the mixing layer commences around 07:00 h. Another single episode of coarse PM_{10} occurred from 10:00 to 20:00 h on 19 March 2006 at CENICA and T0, probably caused by local dust resuspension due to high wind velocity as recorded by Fast et al. (2007) during this day, compared with the rest of the campaign.

4.2 PM composition

As shown in Table 4, TSP, PM_{10} and $PM_{2.5}$ levels in Mexico City are highly influenced by *crustal material* (SiO_2+CO_3^{2-}+Al_2O_3+Ca+Fe+Mg+K): 25–27% of PM_{10} (13–15 $\mu g/m^3$)

in urban sites, and 36 and 43% in the suburban site T1 and at the industrial hotspot Jasso (36 and 27 μg/m^3, respectively); confirming that the high PM_{10} levels recorded at these sites are partly due to dust resuspension. In $PM_{2.5}$ this contribution decreased but still reached relatively high levels (15–28%, 6–9 μg/m^3 at most sites). This crustal influence is also observed when studying the samples under the scanning electron microscope (SEM). Approximately 50% of the particles observed are minerals, mostly silicates (quartz, clays, micas, feldspars, zeolites), but also phosphates, carbonates (calcite and siderite) and sulphates (gypsum).

The *carbonaceous aerosols* also accounted for a high proportion of the PM mass: 23-31% PM_{10} (13–16 μg/m^3, with the highest values for T0) in urban sites, 25 (9–19 μg/m^3) at both industrial influenced sites, and less than 17% (6–10 μg/m^3) in the suburban and rural sites T1 and T2. In $PM_{2.5}$ this contribution increased up to 37% and 23–38% in the urban and suburban and rural sites, respectively, and from 37 to 44% at the industrial sites. The ratio EC/OC in PM_{10} determined in the present study varied from 0.2 to 0.6 for the different sites. An EC/OC ratio of 0.2 for T1 was reported by Doran et al. (2007). The average EC/OC ratio at Tula was 0.4 ($PM_{2.5}$) and 0.3 (PM_{10}), which is consistent with those values reported by Vega et al (2007) for Salamanca (0.4 and 0.3, respectively) which is also an industrial area influenced by a refinery and a power plant.

At the urban sites of CENICA and T0 (PM_{10}), and at the rural site T1 ($PM_{2.5}$) there is a significant correlation of K and OC+EC (R^2=0.4–0.6), but also of K and Al (R^2=0.5–0.8) pointing to the relevance of both biomass combustion and mineral dust (K-feldaspars and illite) emissions contributing to the variability of the levels of these components. The influence of biomass combustion on OC+EC levels also diminishes the typical urban correlation between nitrate and OC+EC levels. Biomass burning episodes and their important influence on PM levels and composition in Mexico were previously reported by Salcedo et al. (2006) and Molina et al. (2007).

Secondary inorganic aerosols (SIA) accounted for 15–20% of PM_{10} and $PM_{2.5}$ mass at the urban sites, 10–19% at the suburban site, and 20–40% at the industrial sites, with

sulfate accounting for around 50–65% of SIA. Levels of ammonium (1.1–1.5 $\mu g/m^3$ in PM_{10}) and sulfate (4–5 $\mu g/m^3$ in PM_{10}) were homogenous at the different urban, suburban and rural sites, and relatively higher at the industrial sites (2.0–2.5 $\mu g NH_4^+/m^3$ and 6.5 $\mu g SO_4^{2-}/m^3$ in PM_{10}). Nitrate levels were relatively low, but higher at the urban sites (2.8–3.6 $\mu g/m^3$ in PM_{10} and $PM_{2.5}$), compared with the suburban and rural (1.1–2.8 $\mu g/m^3$) and industrial (0.6–1.8 $\mu g/m^3$) sites. Levels of SIA in $PM_{2.5}$ were only slightly reduced with respect to PM_{10} for SO_4^{2-} and NO_3^- in the urban sites, but markedly reduced for nitrate in the suburban site T1 (due to the major occurrence of coarser Ca and Na nitrate species). These results coincide with those obtained for $PM_{2.5}$ at the CENICA site during the MCMA-2003 Campaign, when similar levels of sulfate (3.1 $\mu g/m^3$), nitrate (3.7 $\mu g/m^3$) and ammonium (2.2 $\mu g/m^3$) were registered (Salcedo et al., 2006). It is interesting to note that the above described fine PM episodes (overnight trapping of pollutants in Mexico City and during the morning hours) coincide with the peak levels of ammonium sulfate, V and Ni (tracers of fuel-oil combustion and regional/urban background PM climate). Thus, Figs. 7 and 8 show the occurrence of these sulfate-vanadium episodes at CENICA, and Fig. 8 evidences a very good correlation between the levels of the above tracers recorded at CENICA and T0. The levels of most crustal elements and Hg exhibit a good correlation between the two urban sites. Figure 7 also evidences that nitrate and crustal material episodes are recorded during daytime and do not coincide with the above regional episodes, but are more related with local pollution episodes. This is also corroborated by Figure 8, showing lower correlation between levels of nitrate, Ba and Zn (usually associated with road traffic emissions and consequently higher at T0) measured at the two urban sites when compared with sulfate. This is also the case of As and Zr, with relatively higher levels being recorded at CENICA and with a low correlation with T0.

As expected the *marine aerosols* accounted for a very low fraction of PM_{10} (<1.5% in most cases).

As previously reported for PM levels, with the exception of carbonaceous aerosols

and V, levels of major components and *trace elements* in PM are usually much lower (one order of magnitude in some cases) during the MILAGRO campaign than those reported from other large Asian cities (Table 3 and Table 4). Levels in PM_{10} of As (5–7 ng/m^3), Zn (100–500 ng/m^3), Cd (1–3 ng/m^3) and V (20–50 ng/m^3) were relatively high when compared with most urban sites from the US and Europe. However, the limit and target values for Ni, Pb, Cd and As from the EU (1999/30/CE and 2004/107/CE) were met with the exception of As (exceeding slightly the EU target value of 6 ng/m^3). Once again, it is essential to remember that the data obtained during the MILAGRO campaign do not represent annual mean values. The presence of metals in these samples has also been observed in the SEM, with most of them containing Ba (irregular in shape and interpreted as derived from traffic, probably brake linings), Fe (from condensed spherules to amorphous oxidized masses between 1–3 μm in size) or Pb (usually 1 μm or less in size, and commonly spheroidal). Particles of other individual metals are much rarer but include Cu, Zn, Mn, W, Sb, Ni (with V), and Mo, all of which are again very fine grained (usually sub-micron).

According to the above data, PM_{10} at the urban and industrially influenced areas is mainly made up of OC+EC (23–32%), crustal material (25–27% urban, 15–35% industrial) and SIC (15–19% urban, 14–29% industrial). The unaccounted material (mostly water and heteroatoms in organic matter) accounts for 17 to 33% of the PM_{10} mass, whereas the trace elements account for 1 to 2% of the mass. At the rural sites, the proportion of crustal material increases to 32–43%, whereas OC+EC diminishes down to 12-17% (Fig. 9).

In $PM_{2.5}$ (Fig. 9) the crustal material is reduced (but still present in relatively high proportions) in the urban area down to 15% and to 8–17% in the industrially influenced sites, but it is still present in around 30% at the suburban site of T1 due to high local soil resuspension. Conversely, the proportions of carbonaceous aerosols increase up to 37% at the urban and industrial sites and 24% at the suburban site.

As shown in Fig. 10 crustal elements are generally present in the coarse fraction, especially at T1, where they are present in the fraction >10 μm in a significant proportion

ACPD
7, 10589–10629, 2007

EGU

(PM_{10}/TSP ratio 04–0.6). The higher $PM_{2.5}/PM_{10}$ ratios were measured at the urban and industrial sites (0.4 at T0 and Jasso) when compared with the suburban (0.3) site, due to the major anthropogenic origin of the mineral matter in the first locations (road dust, demolition, limestone quarry, cement plants etc). The other elements, mostly with a major anthropogenic origin, are mainly present in the fine fraction, with $PM_{2.5}/PM_{10}$ and PM_{10}/TSP ratios usually >0.6, but in many cases >0.8. However, in some cases, where soil resuspension is important (T1) some elements such as Ni may have an important coarse proportion ($PM_{2.5}/PM_{10}$ and PM_{10}/TSP ratios close to 0.3).

At the urban sites, levels of major and trace crustal components and nitrate were significantly higher during the daylight period than during the night (Fig. 7), by a factor day/night ranging from 1.0 to 1.9 (with the highest values at CENICA) for PM_{10}, as a consequence of higher emissions (from road traffic and from resuspension). Conversely, as shown in Fig. 7, nocturnal levels of sulfate, chloride and most anthropogenic trace elements (Hg, V, Ni, Cu, Zn, As, Se, Mo, Cd, Sn, Ba and Pb) were higher (by a factor of 0.8–1.0, 0.5–0.7 and 0.4–0.9, respectively) probably due, as previously stated, to the reduction of the mixing layer depth. Carbonaceous aerosols increased as a mean also during the night at the urban site T0 by a factor of 1.2 and at the suburban site T1 by a factor of 1.5. At the urban site CENICA day and night levels of these components were very similar.

According to the transport and synoptic scenarios described by Fast et al. (2007) for the MILAGRO campaign, atmospheric transport form Mexico City over the suburban site T1 occurred on 10, 18, 19, 20, 22, and 24 March 2006. From these days sampling took place only during 9–10 and 19–20. As it may be observed in Fig. 11, the atmospheric transport from México City is traced at T1 by the increase of nitrate and potassium in $PM_{2.5}$, whereas the transport from Tula industrial estate is traced by the increase of sulfate levels on 21 March 2006.

4.3 Statistical analysis

Comparing the mean levels of *trace elements* measured at the different study sites in the present work and with the distribution of major PM components, the following source origins may be identified:

- Crustal origin (soil and/or urban dust): Li, Be, P, Sc, Ti, Mn, Co, Ga, Ge, Rb, Sr, Y, Zr, Nb, Cs, Rare Earth Elements, Hf, U, Th.
- Urban (mostly road traffic): Cr, Mn, Cu, Zn, As, Se, Cd, Sn, Sb, Ba and Pb, typically associated with road traffic emissions (engine emissions, abrasion of tyres and brake pads).
- Industrial around Tula: Pb and Cr, V (other elements such as Cd, As, Ni were not analyzed here).
- Industrial and regional (petrochemical estate, fuel oil, petcoke combustion): V, Ni and sulfate.

Particulate Hg is not higher at the urban sites than at the suburban site T1, consequently, as previously reported, it has an external (regional) origin to the city. A possible source for Hg in the area is a city waste incineration power plant as deduced by a previous study of back-trajectories for days with Hg data available (Gonzalez et al., 2007).

These findings were confirmed by performing a statistical analysis of the different datasets, by means of Principal Component Analysis (PCA) with the software STATISTICA v.4.2. This kind of factor analysis requires a minimal internal variability, and therefore it was only applied to the datasets containing >25 samples (CENICA, T0 and T1). PCA was applied separately to the PM_{10} datasets from T0, CENICA and T1, and it was also applied to a larger dataset made up of the combination of the CENICA and T0 samples, with similar results. This confirmed the robustness of the solution.

The results for CENICA were very similar to those for T0, and thus are not included in the description below. At the urban locations (CENICA and T0), four main factors were identified (representing the main source categories):

Factor 1: the main tracers of this factor were Al_2O_3, Ti, Mg, Fe, Ca, P, K, Na, Mn, Th, Ce, Zr, suggesting the clearly mineral origin of this source. This factor probably represents mineral dust resuspension in the city, both road/city and soil dust. The daily evolution of the contribution to the PM mass of this factor showed a marked decrease after 23 March 2006, coinciding with the washout of road and city dust by precipitation.

Factor 2: this factor was characterized by SO_4^{2-}, V, Ni, NH_4^+ and Hg, and it was interpreted as regional-scale transport. The contribution from SO_4^{2-}, NH_4^+ suggests long-range transport, and once again the correlation between these species and Hg is observed and it confirms the regional origin of Hg. The fact that Ni and V are also found in this factor shows that the impact from fuel-oil combustion emissions such as those registered in the Tula industry estate may be detected in Mexico City under specific air mass transport scenarios (regional-scale transport).

Factor 3: Sr, Cu, Ba, Pb, Cr, C, Zn and Cd were the main tracers of this source, which was interpreted as road traffic. SEM-EDX observations confirmed this association of metals. This source was the only one presenting slight differences between T0 and CENICA, probably due to the larger traffic influence in T0. Whereas the factor loadings of major and primary traffic tracers were higher at T0 (C, Cu, Ba, Pb), it was the secondary or minor traffic tracers that were highest at CENICA (NO_3^-, Rb, Cd). This confirms that even though traffic emissions are dominant at both urban sites, their impact is more direct in the case of T0 than of CENICA.

Factor 4: the last factor was characterized by As, Zr, Th, Ce, and Cr, and the nature of this source is yet unclear. This combination of elements could suggest the resuspension of volcanic dust deposited on the city roads, or the influence of an additional source affecting both urban sites.

In the case of the T1 suburban site, five factors were identified:

ACPD
7, 10589–10629, 2007

Factor 1: with Fe, Ti, Mn, Al_2O_3, Ce, Mg, Th, K, Rb, Sr, Ba, Na, Zr, Cr, Ca and P as main tracers, the nature of this source was interpreted as mineral, although some differences may be observed with the mineral source in T0 and CENICA. While the chemical profile in T1 suggests the prevalence of clay minerals, in T0 and CENICA a mixture is observed between clay minerals, carbonates and K-feldspars among others (higher factor loadings for Ca, P, K) originating from construction and demolition activities in the city.

Factor 2: this factor was characterized by Pb, Cd, Cu and Zn and it represents an anthropogenic source of PM, probably linked to industrial emissions which could be related to small smelting plants located to the northeast of Mexico City (R. Moffet, personal communication).

Factor 3: with NH_4^+ and SO_4^{2-} as its main tracers, this source clearly represents regional-scale transport. Hg was also found to correlate with this source, even though the highest factor loading for this element was found in Factor 5.

Factor 4: Sb, As, C, NO_3^- and Cd were the main tracers of this source, which coincided largely with the traffic source at the urban sites. Thus, this source could be interpreted as the contribution from local traffic but also as the transport towards T1 of the emissions from Mexico City. This factor has also high loadings for K and Hg.

Factor 5: V and Ni were the main tracers of this source, which was interpreted as fuel-oil combustion probably from the petrochemical estate in Tula. It is interesting to observe that at T1 the regional source does not include the contributions from V and Ni, which were detected jointly at the urban sites. This indicates that the impact from the emissions from the petrochemical estate is registered at T1 under specific air mass transport scenarios, which do not always coincide with regional-scale transport as in the case of the urban sites.

5 Conclusions

The levels of PMduring the MILAGRO campaign (1 to 31 March 2006) ranged from 50 to 56 μgPM$_{10}$/m^3, 24 to 40 μgPM$_{2.5}$/m^3 and 19 to 33 μgPM$_1$/m^3 in Mexico City. Although these levels may be considered as relatively high when compared with U.S. or European air quality standards, they are markedly lower than PM levels measured at Asian mega-cities.

Daily variations of PM levels were recorded in parallel at the urban sites within the city, despite the distance between the sites (approx. 20 km). This suggests that the variability of PM levels and composition in Mexico City are determined by atmospheric dynamics, more specifically by the mixing layer height, rather than by emission sources. Strong PM peak episodes originated by the decreasing mixing layer height were detected on a number of days between 04:00 and 06:00 h.

Important day-night variations were also observed: the levels of crustal components and NO_3^- presented higher levels during daytime, while SO_4^{2-} concentrations and most of anthropogenic trace metals presented higher levels during night hours.

The analysis of air mass transport scenarios demonstrated the impact of the emissions from Mexico City on the levels and chemical composition of PM on surrounding areas. On days when winds originated from the north/north-west, the impact of the Mexico City plume was clearly detected at the regional background site in Tenango. Conversely, under the influence of winds from the south/south-east, the influence of the Mexico City plume was detected at the T1 site, with nitrate and potassium in PM$_{2.5}$ being identified as major tracers. Finally, westerly circulations evidenced the influence of the emissions from Tula (petrochemical estate) on the chemical composition of PM at T1.

The statistical analysis of the PM$_{10}$ data from T0, CENICA and T1 by PCA resulted in four sources at the urban sites (CENICA and T0), and five sources at the suburban site (T1). At the urban locations the main PM sources were mineral dust (both road/city and soil dust), regional-scale transport (including Hg), traffic emissions and an unidentified

ACPD
7, 10589–10629, 2007

EGU

As source. Traffic emissions were characterized by primary tracers at T0, whereas secondary tracers were highest at CENICA, confirming that the impact of traffic emissions is more direct in T0 than in CENICA. At T1 the main PM sources were mineral dust, industrial emissions, regional-scale transport, local traffic (also interpreted as the transport towards T1 of the emissions from Mexico City), and oil combustion originating probably from the petrochemical estate in Tula. The interpretation of the traffic source at all sites was confirmed by the observation of Ba, Fe, Cu and Pb particles by SEM-EDX.

Acknowledgements. This study was supported by the Acción Complementaria from the Ministry of Education and Science of Spain CGL2005-23745-E. We also thank the support from the Spanish Ministry of the Environment. We would like also to thank W. Eichinger from the University of Iowa for making available the meteorological data at T0 during the campaign.

References

Balachandran, S., Meena, B. R., and Khillare, P. S.: Particle size distribution and its elemental composition in the ambient air of Delhi, Environment International 26, 49–54, 2000.

Bogo, H., Otero, M., Castro, P., Ozafrán, M. J., Kreiner, A., Calvo, E. J., and Negri, R. M.: Study of atmospheric particulate matter in Buenos Aires city, Atmos. Environ., 37, 1135–1147, 2003.

Chan, C. Y., Xu, X. D., Li, Y. S., Wong, K. H., Ding, G. A., Chan, L. Y., and Cheng, X. H.: Characteristics of vertical profiles and sources of PM2.5, P M10 and carbonaceous species in Beijing, Atmos. Environ., 39, 5113–5124, 2005.

CAFE: Clean Air for Europe: European Commission. Second Position Paper on Particulate Matter – CAFE Working Group on Particulate Matter, D.G. Environment. April 2004, 234 pp, 2004.

Clean Air Initiatives for Asian cities, 2006. Air Quality in Asian cities, 6 p., http://www.cleanairnet.org/caiasia/1412/article-59689.html.

Dockery, D., Pope, C., Xu, X., Spengler, J., Ware, J., Fay, M., Ferris, B., and Speizer, F.: An association between air pollution and mortality in six US cities, New England Journal of Medicine, 329, 1753–1759, 1993.

Doran, J. C., Arnott, W. P., Barnard, J. C., Cary, R., Coulter, R., Fast, J. D., Kassianov, E. I., Kleinman, L., Laulainen, N. S., Martin, T., Paredes-Miranda, G., Pekour, M. S., Shaw, W. J., Smith, D. F., Springston, S. R., and Yu X.-Y.: The T1-T2 study: evolution of aerosol properties downwind of Mexico City, Atmos. Chem. Phys., 7, 1585–1598, 2007, http://www.atmos-chem-phys.net/7/1585/2007/.

Fast J. D. and Zhong, S.: Meteorological factors associated with inhomogeneous ozone concentrations within the Mexico City basin, J. Geophys. Res., 103, 18 927–18 946, 1998.

Fast, J. D., de Foy, B., Acevedo Rosas, F., Caetano, E., Carmichael, G., Emmons, L., McKenna, D., Mena, M., Skamarock, W., Tie, X., Coulter, R. L., Barnard, J. C., Wiedinmyer, C., and Madronich, S.: A meteorological overview of the MILAGRO field campaigns, Atmos. Chem. Phys., 7, 2233–2257, 2007, http://www.atmos-chem-phys.net/7/2233/2007/.

Fung, K., Chow, J., and Watson, J.: Evaluation of OC/EC Specition by Thermal Manganese Dioxide Oxidation and the IMPROVE Method, Air Waste Manage. Assoc., 52, 1333–1341, 2002.

González, R., Márquez, C., Bernabé, R., Snyder, D. C., Rutter, A. P., Minguillón, M. C., Pérez, N., Pey, J., Alverdin, L., Reyes, E., Miranda, L., Miranda, J., Moreno, T., Blanco, S., De la Rosa, A., Solórzano, G., Alastuey, A., Schauer, J., Querol, X., de Foy, B., Molina, L. T., and Cárdenas, B.: A43A-20 Measurements of Total Gaseous and Particulate Mercury in Mexico City During the MCMA-2006/MILAGRO Campaign. Proceedings of the Joint Assembly of the American Geophysical Union (AGU 2007). Acapulco, Mexico, 22-25 May 2007.

Hea, K., Yang, F., Ma, Y., Zhang, Q., Yao, X., Chan, Ch. K., Cadle, S., Chan, T., and Mulawa, P.: The characteristics of PM2.5 in Beijing, China, Atmos. Environ., 35, 4959–4970, 2001.

Ho, K. F., Lee, S. C., Chan, C. K., Yu, J. C., Chow, J. C., and Yao, X. H.: Characterization of chemical species in PM2.5 and PM10 aerosols in Hong Kong, Atmos. Environ., 37, 31–39, 2003.

Karar, K. and Gupta, A. K.: Source apportionment of PM10 at residential and industrial sites of an urban region of Kolkata, India, Atmos. Res., 84, 30–41, 2007.

Kim, K.-H. and Kim M.-Y.: The effects of Asian Dust on particulate matter fractionation in Seoul, Korea during spring 2001, Chemosphere 51, 707–721, 2003.

Künzli, N., Kaiser, R., Medina, S., Studnicka, M., Chanel, O., Filliger, P., Herry, M., Horak Jr, F., Puybonnieux-Texier, V., Quénel. P., Schneider, J., Seethaler, R., Vergnaud, J.-C., and Sommer, H.: Public health impact of outdoor and traffic-related air pollution: a tri-national

European assessment, Lancet, 356, 795–801, 2000.
Kumar, A. V., Patil, R. S., and Nambi, K. S. V.: Source apportionment of suspended particulate matter at two traffic junctions in Mumbai, India, Atmos. Environ., 35, 4245–4251, 2001.
Molina, L. T., Kolb, C. E., de Foy, B., Lamb, B. K., Brune, W. H., Jimenez, J. L., Ramos-Villegas, R., Sarmiento, J., Paramo-Figueroa, V. H., Cardenas, B., Gutierrez-Avedoy, B., and Molina, M. J.: Air quality in North America's most populous city – overview of the MCMA-2003 campaign, Atmos. Chem. Phys., 7, 2447–2473, 2007, http://www.atmos-chem-phys.net/7/2447/2007/.
Mönkkönen, P., Uma, R., Srinivasan, D., Koponen, I. K., Lehtinen, K. E. J., Hämeri, K., Suresh, R., Sharma, V. P., and Kulmala, M.: Relationship and variations of aerosol number and PM10 mass concentrations in a highly polluted urban environment—New Delhi, India, Atmos. Environ., 38, 425–433, 2004.
Querol, X., Alastuey, A., Rodríguez, S., Plana, F., Ruiz, C. R., Cots, N., Massagué, G., and Puig, O.: PM10 and PM2.5 source apportionment in the Barcelona Metropolitan Area, Catalonia, Spain, Atmos. Environ., 35/36, 6407-6419, 2001.
Rojas-Bracho, L., Suh, H. H., Oyola, P., and Koutrakis, P.: Measurements of children's exposures to particles and nitrogen dioxide in Santiago, Chile, The Science of The Total Environment, 287, 3, 249–264, 2002.
Salcedo, D., Onasch, T. B., Dzepina, K., Canagaratna, M. R., Zhang, Q., Huffman, J. A., DeCarlo, P. F., Jayne, J. T., Mortimer, P., Worsnop, D. R., Kolb, C. E., Johnson, K. S., Zuberi, B., Marr, L. C., Volkamer, R., Molina, L. T., Molina, M. J., Cardenas, B., BernabÉ, R. M., Márquez, C., Gaffney, J. S, Marley, N. A., Laskin, A., Shutthanandan, V., Xie, Y., Brune, W., Lesher, R., Shirley, T., Jimenez, J. L.: Characterization of ambient aerosols in Mexico City during the MCMA-2003 campaign with Aerosol Mass Spectrometry: results from the CENICA Supersite, Atmos. Chem. Phys., 6, 925–946, 2006, http://www.atmos-chem-phys.net/6/925/2006/.
Sun, Y., Zhuang, G., Wang, Y., Han, L., Guo, J., Dan, M., Zhang, W., Wang, Z., and Hao, Z.: The air-borne particulate pollution in Beijing concentration, composition, distribution and sources, Atmos. Environ., 38, 5991–6004, 2004.
Vega, E., Reyes, E., Ruiz, H., Garcia, J., Sanchez, G., Martinez-Villa, G., and Gonzalez, U.: Analysis of PM2.5 and PM10 in the atmosphere of Mexico City during 2000–2002, J. Air Waste Manage. Assoc., 54(7), 786–798, 2004.
Vega, E., Ruiz, H., Martinez-Villa, G., Sanchez, G., Sosa, G., Gonzalez-Avalos, E., Reyes, E.,

and Garcia, J.: Fine and Coarse Particulate Matter Chemical Characterization in a Heavily Industrialized City in Central Mexico during Winter 2003, J. Air Waste Manage. Assoc., 57, 620–633, 2007.

Volkamer, R., Jimenez, J. L., SanMartini, F., Dzepina, K., Zhang, Q., Salcedo, D., Molina, L. T., Worsnop, D. R., Molina, M. J.: Secondary organic aerosol formation from anthropogenic air pollution: Rapid and higher than expected, Geophys. Res. Lett., 33, L17811, doi:10.1029/2006GL026899, 2006.

Wang, G., Wang, H., Yu, Y., Gao, Sh., Feng, J., Gao, S., and Wang, L.: Chemical characterization of water-soluble components of PM10 and PM2.5 atmospheric aerosols in five locations of Nanjing, China, Atmos. Environ., 37, 2893–2902, 2003.

WHO: Health aspects of air pollution with particulate matter, ozone and nitrogen dioxide. World Health Organization. Report EUR/03/5042688, 98 pp., 2003.

WHO: World Health Organization air quality guidelines global update 2005, 25 pp., 2005.

WHO/UNEP: Urban Air Pollution in Megacities of the World. Blackwell, Oxford, 1992.

Zhang, Q., Jimenez, J. L. Canagaratna, M. R., Allan, J. D., Coe, H., Ulbrich, I., Alfarra, M. R., Takami, A., Middlebrook, A. M., Sun, Y. L., Dzepina, K., Dunlea, E., Docherty, K., DeCarlo, P. F., Salcedo, D., Onasch, T., Jayne, J. T., Miyoshi, T., Shimono, A., Hatakeyama, S., Takegawa, N., Kondo, Y., Schneider, J., Drewnick, F., Borrmann, S., Weimer, S., Demerjian, K., Williams, P., Bower, K, Bahreini, R., Cottrell, L., Griffin, R. J., Rautiainen J., Sun, J. Y., Zhang, Y. M., and Worsnop, D. R.: Ubiquity and dominance of oxygenated species in organic aerosols in anthropogenically-influenced Northern Hemisphere midlatitudes, Geophys. Res. Lett., 34, L13801, doi:10.1029/2007GL029979, 2007.

Zheng, J., Tan, M., Shibata, Y., Tanaka, A., Li, Y., Zhang, G., Zhang, Y., and Shan, Z.: Characteristics of lead isotope ratios and elemental concentrations in PM10 fraction of airborne particulate matter in Shanghai after the phase-out of leaded gasoline, Atmos. Environ., 38, 1191–1200, 2004.

Table 1. Location of the monitoring stations.

Site	Coordinates			Type of site
UNAM	19°19′ 31″ N	99°10′ 51″ W	2220 m a.s.l.	urban background
CENICA	19°21′ 32″ N	99°04′ 25″ W	2232 m a.s.l.	urban background
T0	19°29′ 22″ N	99°08′ 22″ W	2243 masl	urban background
T1	19°42′ 14″ N	98°57′ 45″ W	2270 m a.s.l.	suburban
T2	20°01′ 14″ N	98°54′ 09″ W	2542 m a.s.l.	rural
Tenango	19°09′ 18″ N	98°51′ 50″ W	2377 m a.s.l.	rural
Corena	19°15′ 52″ N	99°18′ 07″ W	2300 m a.s.l.	urban background
Jasso	20°01′ 02″ N	99°18′ 55″ W	2125 m a.s.l.	industrial hotspot
PXT	19°51′ 44″ N	99°17′ 43″ W	2329 m a.s.l.	rural closet o industry

Table 2. Mean TSP, PM_{10}, $PM_{2.5}$ and PM_1 ($\mu g/m^3$) levels obtained at the different monitoring stations, for the periods indicated.

Location		n (TSP, PM_{10}, $PM_{2.5}$)	TSP	PM_{10}	$PM_{2.5}$	PM_1
Real time measurements						
CENICA	08-29/03/06		144	50	24	19
T0	19-30/03/06			56	40	33
Tenango	28/03/06-06/04/06			22	13	10
Corena	01-04/04/06			30	25	17
PM samplers (gravimetry)						
CENICA	01/03/06 to 06/04/06	38		53		
T0	01/03/06 to 06/04/06	37, 27		50	40	
T1	01-29/03/06	23, 24, 25	193	80	33	
UNAM	01-15/03/06	7		54		
T2	09-17/03/06	8		34		
Tula- PXT	24/03/06-20/04/06	28, 42		37	26	
Tula- Jasso	24/03/06-20/04/06	28, 42		75	31	

ACPD
7, 10589–10629, 2007

Table 3. Mean PM_{10} and $PM_{2.5}$ levels and PM_{10} speciation from large Asian cities compared with the data obtained in this study for Mexico City.* Only water soluble fraction. [a]Kim and Kim (2003); [b]Clean Air Initiatives for Asian cities (2006). Air Quality in Asian cities, 6 p. http://www.cleanairnet.org/caiasia/1412/article-59689.html;[c]Zheng et al. (2004); [d]Hea et al. (2001); [e]Chan et al. (2005); [f]Ho et al. (2003); [g]Sun et al. (2004); [h]Wang et al. (2003), [i]Karar et al. (2007), [j]Mönkkönen et al. (2004); [k]Balachandran et al. (2000); [l]Kumar et al. (2001); [m]Rojas-Bracho et al. (2002), [n]Bogo et al. (2003). NR. Not reported.

	Seoul[a]	Tokyo[b]	Taiwan[b]	China[c--g]		China[h]	Calcutta[i]		New Delhi[j,k]	Mumbai[l]	S. de Chile[m]	Buenos Aires[n]	Sao Paulo[m]	Mexico This study	
$\mu g/m^3$				min	max	Nanjing	min	max						CENICA	T0
$PM_{2.5}$	56	NR	NR	50	127	222	NR	NR	NR	NR	68	35	35	24	46
PM_{10}	109	35	NR	79	197	317	140	197	278	NR	115	50	77	52	52
OC+EC	NR	NR	NR	14	31	29*	2	3	NR	NR	NR	NR	NR	14	16
Al_2O_3	NR	NR	NR	5	11	NR	NR	NR	NR	NR	NR	NR	NR	3	2
Ca	NR	1	2	2	10	5*	NR	NR	NR	NR	NR	NR	NR	1	2
Fe	NR	1	1	1	3	NR	0.1	0.1	NR	NR	NR	NR	NR	1	1
K	NR	0.4	1	2	4	3*	NR	NR	NR	NR	NR	1	NR	1	1
Mg	NR	0.2	1	1	2	1*	NR	NR	NR	NR	NR	NR	NR	0.5	0.4
Na	NR	1	8	1	8	4*	NR	NR	NR	NR	NR	2	NR	0.5	0.5
SO_4^{2-}	NR	NR	10	15	30	18	1	2	NR	NR	NR	7	NR	5	5
NO_3^-	NR	NR	NR	3	20	9	0.2	0.2	NR	NR	NR	4	NR	4	4
Cl^-	NR	NR	NR	1	5	2	1	1	NR	NR	NR	5	NR	1	1
NH_4^+	NR	NR	NR	4	13	11	NR	NR	NR	NR	NR	3	NR	2	2
ng/m^3															
As	NR	2	50	6	66	NR	NR	NR	NR	6	NR	NR	NR	5	6
Cr	NR	6	20	6	40	NR	7	6	280	100	NR	NR	NR	1	4
Zn	NR	233	380	295	1409	NR	490	535	600	NR	NR	NR	NR	100	482
Sr	NR	NR	10	30	40	NR	NR	NR	NR	NR	NR	NR	NR	9	16
Pb	NR	64	90	82	409	NR	40	120	660	900	NR	NR	NR	32	111
Ni	NR	5	50	4	75	NR	7	8	250	160	NR	NR	NR	3	5
Co	NR	1	–	1	5	NR	NR	NR	NR	NR	NR	NR	NR	0.5	1
Cd	NR	2	10	9	11	NR	2	5	80	NR	NR	NR	NR	1	3
Mn	NR	30	70	23	186	NR	2	2	NR	860	NR	NR	NR	20	32
V	NR	6	10	5	18	NR	NR	NR	NR	NR	NR	NR	NR	19	25
Cu	NR	27	250	40	170	NR	NR	NR	NR	900	NR	NR	NR	75	110
Ti	NR	40	NR	80	285	NR	NR	NR	NR	NR	NR	NR	NR	114	81

ACPD
7, 10589–10629, 2007

EGU

Table 4. Mean TSP, PM_{10} and $PM_{2.5}$ levels and major components ($\mu g/m^3$) recorded at the study sites during the MILAGRO campaign.

	CENICA	T0			T1		T2	UNAM	Jasso		PXT	
	PM_{10}	$PM_{2.5}$	PM_{10}	$PM_{2.5}$	PM_{10}	PST	PM_{10}	PM_{10}	PM_{10}	$PM_{2.5}$	PM_{10}	$PM_{2.5}$
n	38	27	36	25	24	23	8	7	28	28	27	27
PM	53	40	50	33	82	193	34	54	75	31	37	26
OC	10.8	12.4	12.9	3.7	5.0	8.0	ND	8.0	12.9	8.0	7.1	8.0
EC	3.6	2.1	2.7	4.0	5.3	5.6	ND	4.7	6.0	3.6	2.2	3.4
CO_3^{2-}	2.0	0.9	2.3	1.1	4.2	9.2	1.3	2.3	13.8	2.5	1.4	0.5
SiO_2	5.1	2.4	4.9	4.0	15.7	34.6	4.7	5.6	2.4	0.6	1.4	0.9
Al_2O_3	2.5	1.2	2.4	2.0	7.9	17.3	2.3	2.8	0.6	0.1	0.4	0.1
Ca	1.3	0.6	1.5	0.7	2.8	6.2	0.9	1.5	9.2	1.7	0.9	0.3
K	0.7	0.3	0.7	0.6	1.1	1.9	0.5	0.6	0.2	0.1	0.1	0.2
Na	0.5	0.3	0.5	0.3	0.8	1.6	0.2	0.4	0.2	0.1	0.1	0.1
Mg	0.5	0.1	0.4	0.3	0.9	1.8	0.3	0.4	0.3	0.1	0.1	0.04
Fe	0.9	0.4	1.1	0.6	2.0	4.2	0.6	1.0	0.6	0.1	0.6	0.2
SO_4^{2-}	4.9	3.7	5.3	3.9	4.8	6.3	4.4	4.2	6.4	3.7	6.4	6.4
NO_3^-	3.5	2.8	3.6	1.1	2.8	4.2	1.2	1.8	1.8	0.6	1.6	0.8
Cl^-	0.4	0.7	0.4	0.2	0.3	0.5	0.1	0.1	0.1	0.2	0.1	0.1
NH_4^+	1.6	1.0	1.5	1.1	1.1	1.2	1.2	1.5	2.0	1.6	2.4	2.5

ACPD
7, 10589–10629, 2007

Table 5. Mean levels of trace components in TSP, PM_{10} and $PM_{2.5}$ (ng/m^3) recorded at the study sites during the MILAGRO campaign. NA: not available.

	CENICA	T0			T1		T2	UNAM	Jasso		PXT	
	PM_{10}	PM_{10}	$PM_{2.5}$	TSP	PM_{10}	$PM_{2.5}$	PM_{10}	PM_{10}	PM_{10}	$PM_{2.5}$	PM_{10}	$PM_{2.5}$
n	38	36	27	23	24	25	8	7	28	28	27	27
Hg	0.14	0.22	0.13	0.40	0.28	0.18	0.04	0.11	NA	NA	NA	NA
Li	0.4	0.5	0.4	2.2	1.0	0.2	0.1	0.5	NA	NA	NA	NA
Be	0.05	0.05	0.04	0.57	0.27	0.12	0.05	0.05	NA	NA	NA	NA
P	100	120	53	304	166	48	72	106	NA	NA	NA	NA
Sc	0.6	0.6	0.5	1.6	1.0	0.5	0.2	1.1	NA	NA	NA	NA
Ti	109	81	36	440	205	57	65	85	NA	NA	NA	NA
V	19	25	13	27	17	10	9	16	50	30	21	18
Cr	0.7	4.4	2.1	4.9	1.5	0.9	0.1	1.9	20	15	192	102
Mn	20	32	16	83	41	13	15	23	NA	NA	NA	NA
Co	0.5	0.8	0.5	1.6	0.9	0.2	0.3	0.5	NA	NA	NA	NA
Ni	3	5	3	9	5	2	1	3	NA	NA	NA	NA
Cu	78	110	90	103	33	27	13	140	13	11	10	5
Zn	103	482	244	187	165	97	8	98	21	11	11	5
Ga	0.4	0.4	0.3	1.9	1.2	0.4	0.4	0.1	NA	NA	NA	NA
Ge	< 0.1	0.2	0.2	0.3	0.1	0.1	< 0.1	< 0.1	NA	NA	NA	NA
As	6	6	6	4	3	2	1	7	NA	NA	NA	NA
Se	7	6	6	3	3	3	1	7	NA	NA	NA	NA
Rb	0.9	0.9	0.5	2.5	1.8	1.0	0.6	0.7	NA	NA	NA	NA
Sr	9	16	5	38	18	5	5	9	NA	NA	NA	NA
Y	0.3	0.2	0.1	1.8	0.9	0.2	0.1	0.2	NA	NA	NA	NA
Zr	20	18	15	45	29	22	6	23	NA	NA	NA	NA
Nb	0.4	0.4	0.3	1.9	1.1	0.4	0.3	0.5	NA	NA	NA	NA
Mo	1	2	2	8	5	3	0.1	0.1	NA	NA	NA	NA
Cd	2	3	3	1	1	1	0.3	2	NA	NA	NA	NA
Sn	23	32	29	12	14	9	4	7	NA	NA	NA	NA
Sb	15	16	15	10	10	8	3	8	NA	NA	NA	NA
Cs	0.1	0.1	0.1	0.3	0.2	0.1	< 0.1	0.2	NA	NA	NA	NA
Ba	30	92	22	82	43	12	3	27	NA	NA	NA	NA
La	1.3	0.8	0.7	0.4	1.2	0.5	0.7	0.5	NA	NA	NA	NA
Ce	1.6	1.5	1.2	6.9	4.1	1.1	1.0	1.5	NA	NA	NA	NA
Hf	0.7	0.6	0.5	1.4	0.9	0.7	0.2	0.8	NA	NA	NA	NA
Tl	0.6	0.4	0.3	0.3	0.5	0.2	< 0.1	0.3	NA	NA	NA	NA
Pb	34	111	62	35	31	23	6	26	23	20	253	199
Bi	0.2	0.4	0.3	0.3	0.1	0.1	0.2	0.2	NA	NA	NA	NA
Th	0.1	0.1	0.1	1.1	0.5	0.1	0.1	0.2	NA	NA	NA	NA
U	0.3	0.3	0.2	0.5	0.4	0.4	0.2	0.4	NA	NA	NA	NA

ACPD

7, 10589–10629, 2007

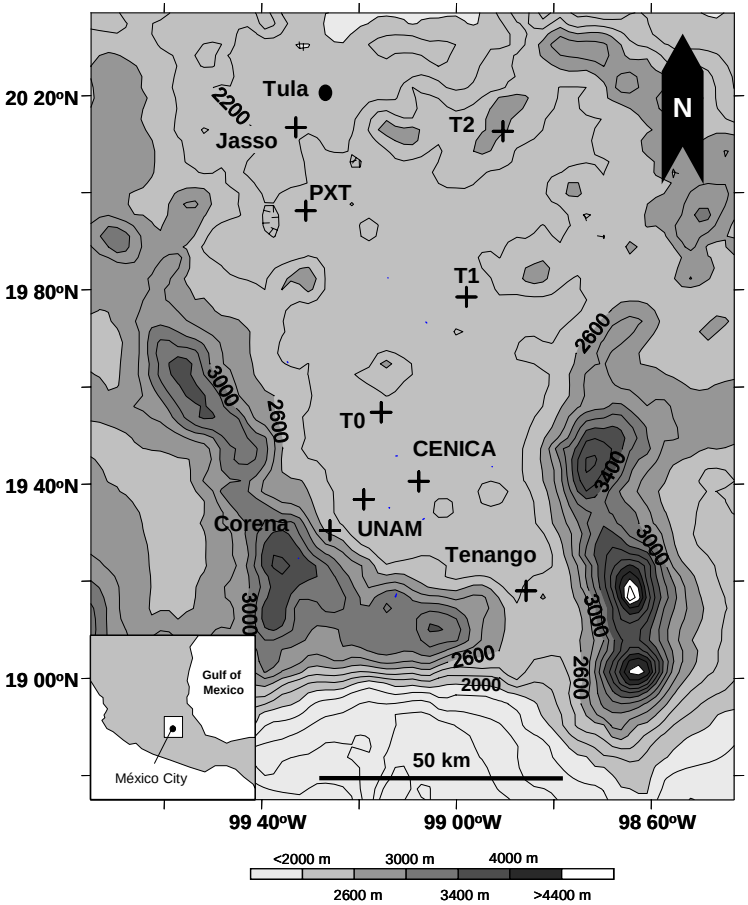

Fig. 1. Location of the PM monitoring sites in and around Mexico City and the Tula petrochemical estate.

ACPD
7, 10589–10629, 2007

EGU

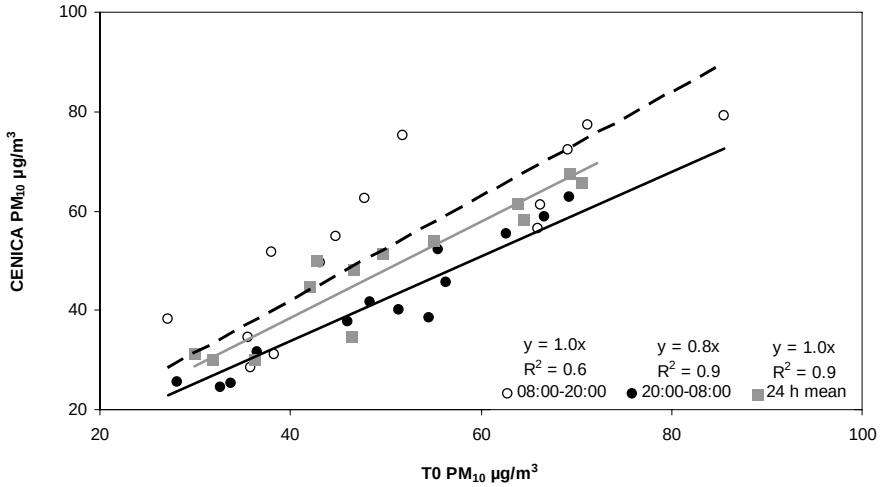

Fig. 2. Comparison of 12 and 24 h PM_{10} levels simultaneously measured at T0 and CENICA (two urban background sites), Mexico City, during the MILAGRO campaign.

ACPD
7, 10589–10629, 2007

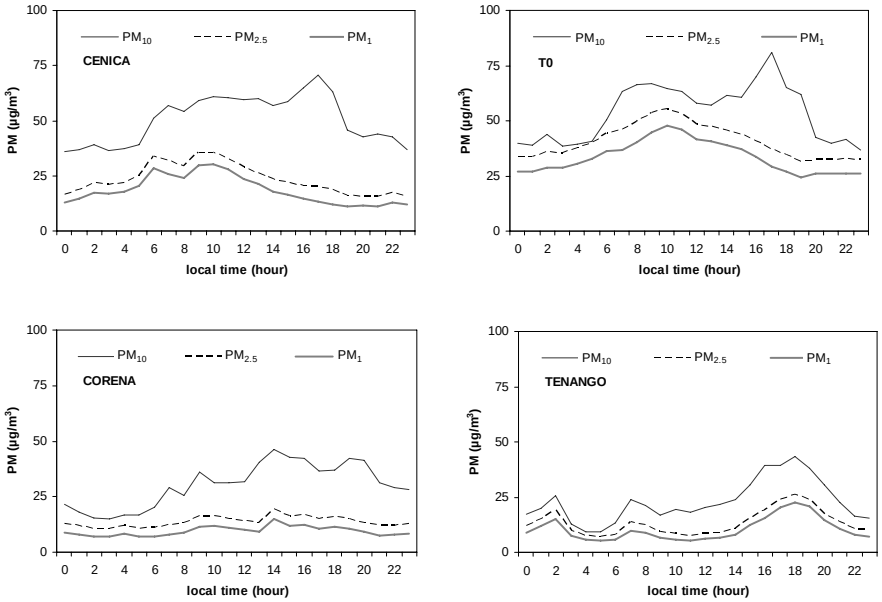

Fig. 3. Mean hourly PM levels measured during the whole MILAGRO campaign at 2 urban background sites of Mexico City, CENICA and T0, and at two southern sites, Tenango and Corena.

ACPD
7, 10589–10629, 2007

EGU

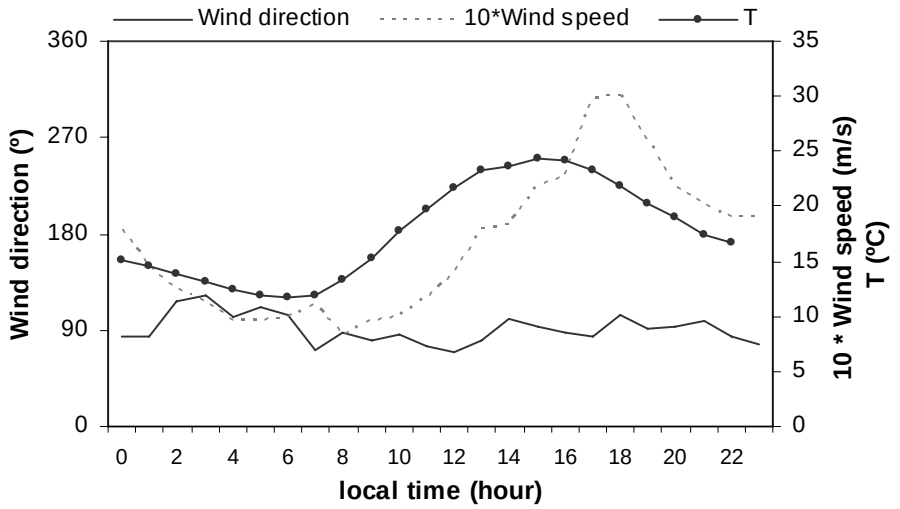

Fig. 4. Mean hourly temperature, wind direction and wind speed recorded at T0 from 1 to 26 March 2006.

ACPD
7, 10589–10629, 2007

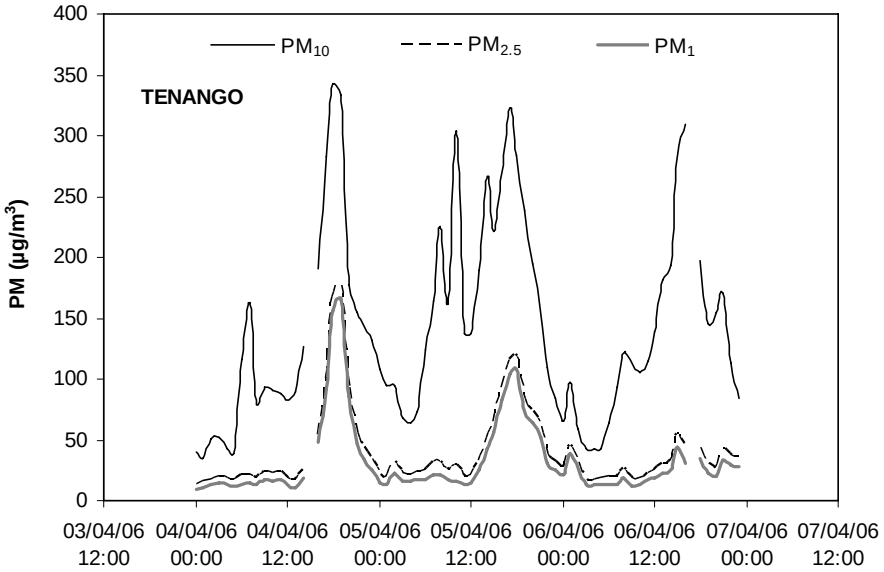

Fig. 5. Hourly PM levels measured at the rural site Tenango, showing the Mexico City's plume impact causing high levels of PM_1.

ACPD
7, 10589–10629, 2007

EGU

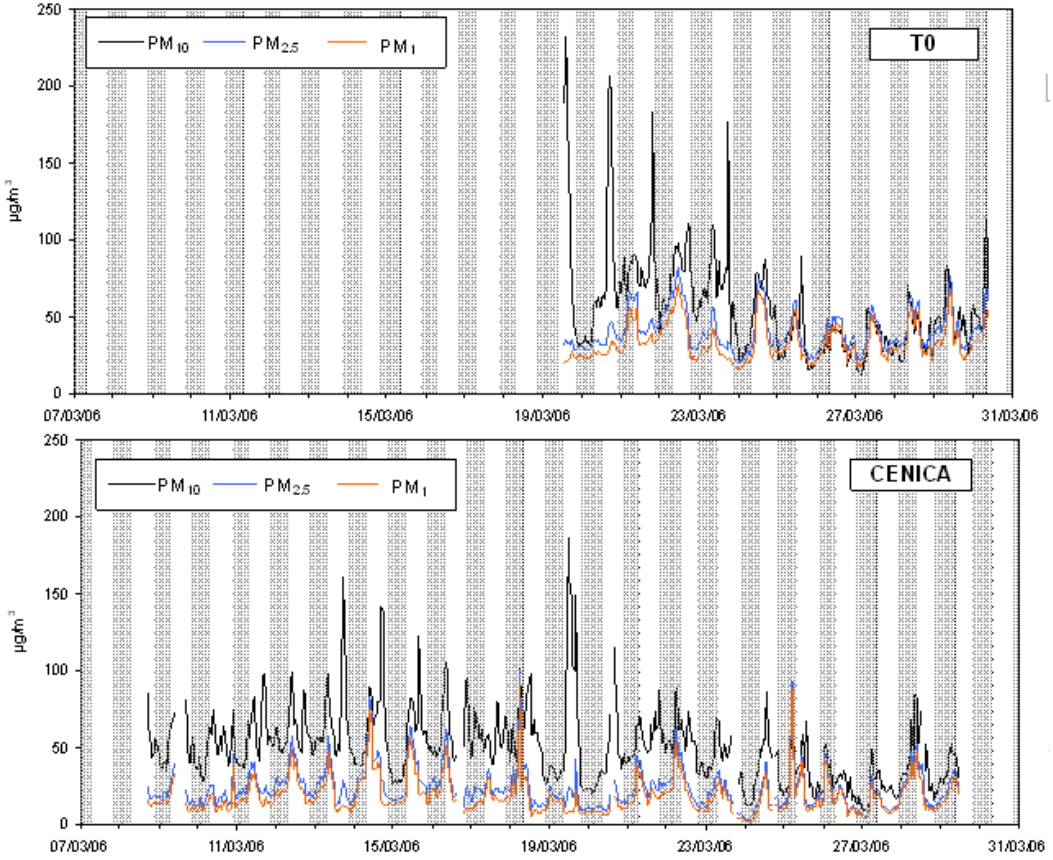

Fig. 6. Hourly PM levels measured during the whole MILAGRO campaign at 2 urban background sites of Mexico City, CENICA and T0.

ACPD
7, 10589–10629, 2007

EGU

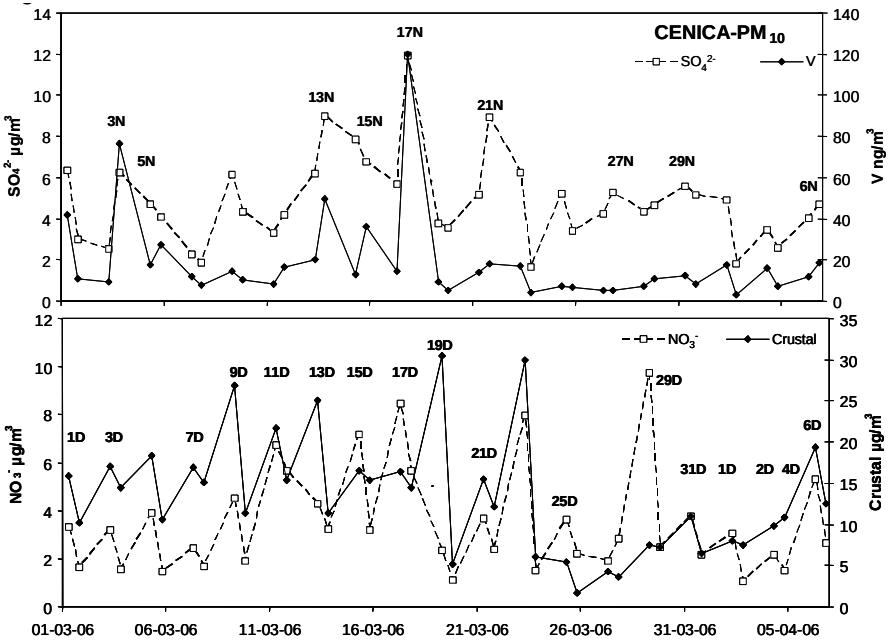

Fig. 7. Mean 12 h levels of SO_4^{2-}, NO_3^-, V and crustal material recorded at CENICA during the MILAGRO campaign. N, maximum value recorded in the nighttime sample; D maximum value recorded in the daylight sample.

ACPD
7, 10589–10629, 2007

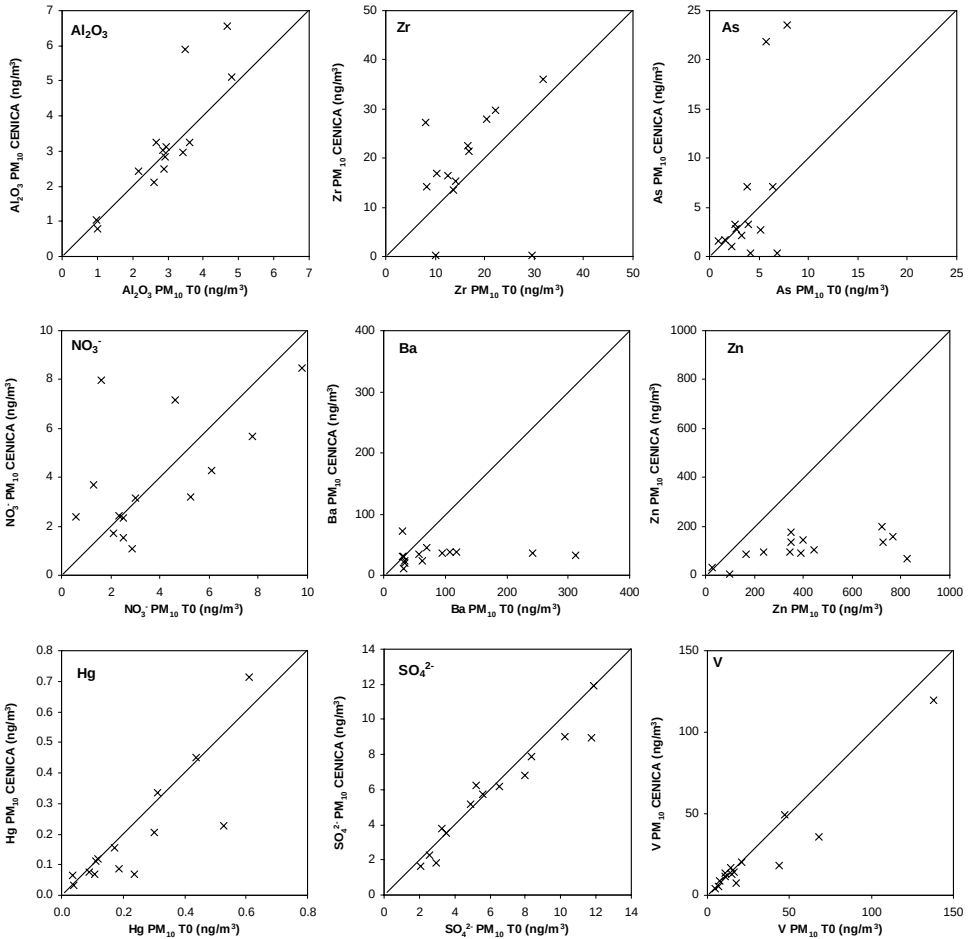

Fig. 8. Correlation between levels of Al_2O_3, Zr, As, NO_3^-, Ba, Zn, Hg, V and SO_4^{2-} in PM_{10} at CENICA and T0.

ACPD
7, 10589–10629, 2007

EGU

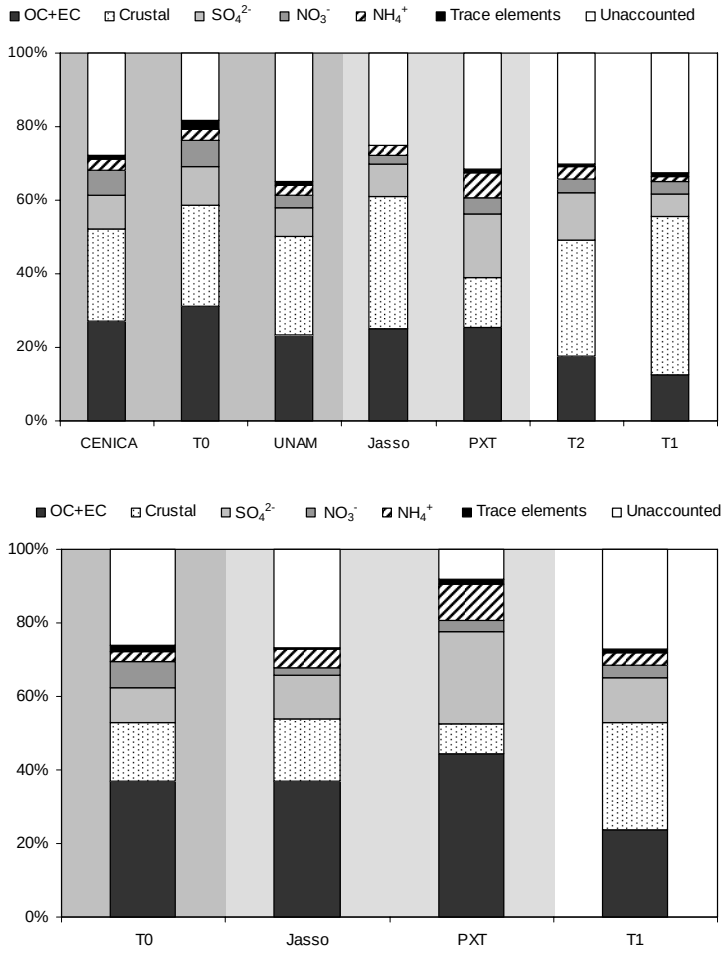

Fig. 9. Mean PM_{10} (top) and $PM_{2.5}$ (bottom) composition obtained at urban (grey dark), industrial-rural (gray clear) and suburban and rural rural sites.

ACPD
7, 10589–10629, 2007

PM speciation and sources in Mexico during MILAGRO campaign

X. Querol et al.

EGU

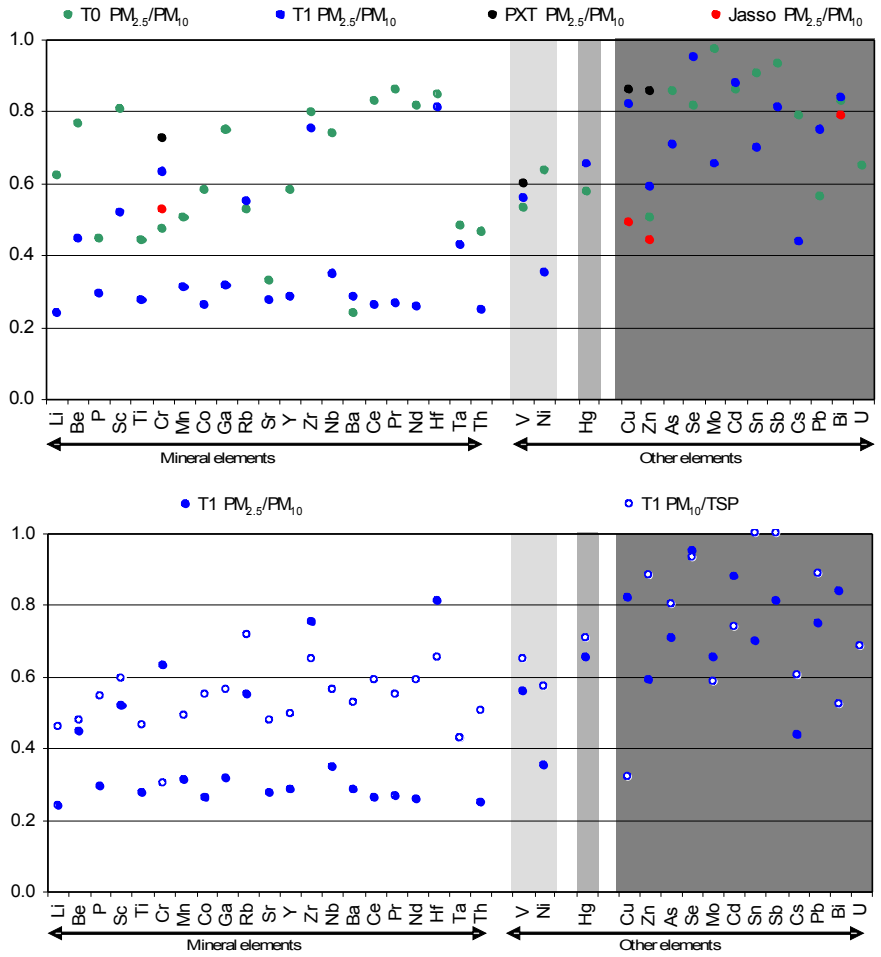

Fig. 10. $PM_{2.5}/PM_{10}$ ratios of trace elements levels at T0, T1, Jasso and PXT. PM_{10}/TSP levels at T1.

ACPD
7, 10589–10629, 2007

PM speciation and sources in Mexico during MILAGRO campaign

X. Querol et al.

EGU

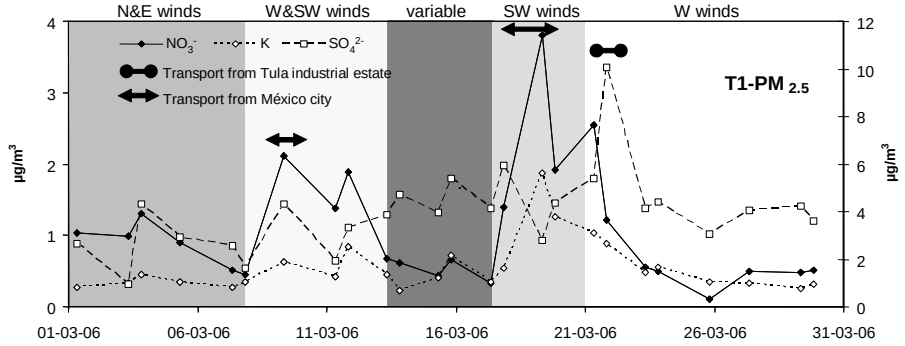

Fig. 11. 12 h levels (daylight and night) of nitrate, potassium and sulfate in $PM_{2.5}$ measured at the T1 suburban site on 1, 3, 5, 7, 9, 11, 13, 16, 17, 19, 21, 23, 25, 27 and 29 March 2006. Note that nitrate and potassium trace the transport from México City, whereas sulfate is mainly tracing the transport from Tula industrial estate. The transport and synoptic scenarios described by Fast et al. (2007) for the MILAGRO campaign are also marked in the plot.

ACPD
7, 10589–10629, 2007

EGU